# Energy & Environmental Science

Accepted Manuscript






ROYAL SOCIETY OF CHEMISTRY

www.rsc.org/ees

Energy & Environmental Science

RSCPublishing

ARTICLE

# The Photobioelectrochemical Activity of Thylakoid Bioanodes is Increased *via* Photocurrent Generation and Improved Contacts by Membrane-Intercalating Conjugated Oligoelectrolytes†

RightCite this: DOI: 10.1039/x0xx00000x

Received 00th January 2012,
Accepted 00th January 2012

DOI: 10.1039/x0xx00000x

www.rsc.org/

Nathan D. Kirchhofer,[§,a] Michelle A. Rasmussen,[§,b] Frederick W. Dahlquist,[c] Shelley D. Minteer,*[b] and Guillermo C. Bazan*[a,c,d]

The photobioelectrochemical impact of a series of conjugated oligoelectrolytes (COEs) with a systematic progression of chemical structures was elucidated by their direct incorporation into thylakoid bioanodes. In both three-electrode electrochemical cells and bio-solar cell devices, significant anodic performance enhancements ($p < 0.1$) were observed when anodes were modified with certain COEs. Amperometric photocurrent densities increased by up to 2.3-fold for the best COE. In bio-solar cell devices, short-circuit photocurrent increased by up to 1.7-fold and short-circuit dark current increased by up to 1.4-fold, indicating that the best COEs enhance both photocurrent generation and interfacial electron transfer. Trends in these results indicate that the molecular length and pendant charge of COEs differentially contribute to photobioelectrochemical enhancements, and the optimal combination of these features is revealed. Control experiments indicate that COEs augment native thylakoid functionality, as COEs do not have redox activity or undergo chemical degradation.

Broader Impact: Conjugated oligoelectrolytes (COEs)—water soluble organic semiconducting oligomers with high membrane affinity—are able to modulate biocurrent in various dark-current microbial bioelectrochemical systems. In these systems, COE molecules boost native microbial transmembrane charge transfer processes. However, COEs have not been exploited for energy harvesting/transfer purposes in practical light-driven biosystems such as thylakoid-based bio-solar cells, self-powered bio- or photo-sensors, and biotransistors. For the first time, we show that COE additives significantly enhance the performance of thylakoid-based devices. The best COEs improve both the dark- and photo-current output of thylakoid bioanodes, implicating a synergistic improvement of electrode contacts and photocurrent generation, and trends in these results reveal key structure-property relationships that guide future use.

## Introduction

Investigations[1–8] of membrane-intercalating conjugated oligoelectrolytes (COEs), such as those in Fig. 1, have largely focused on microbial bioelectrochemical systems in the absence of illumination. One study[9] with an illuminated synthetic photovoltaic system reported >93% efficient transmembrane Förster resonance energy transfer[10] (FRET) from COE1-4C (a.k.a. DSSN+) to gold-electrode-tethered Nile red, and this enabled a 36% higher photocurrent density to be generated upon white light irradiation. COE1-4C was selected for its lipid-phase photoluminescence (PL) spectral overlap with Nile red's absorption; this is feasible because COE1-type molecules' absorption onset (optical gap) and PL are red-shifted relative to COE2-type analogues (Fig. S1), due to D-A-D character.[11–13]

The Nile red synthetic photovoltaic system represents an analogue of the thylakoid membrane of green plants—the most

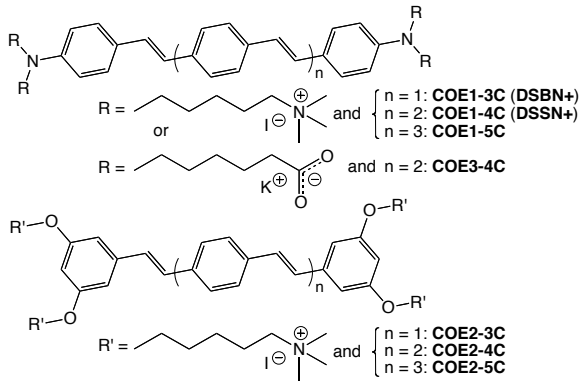


Fig. 1. The seven COE derivatives used in this study. Note that COE1-3C and COE1-4C may also be referred to as DSBN+ and DSSN+, respectively, as seen previously in the literature.

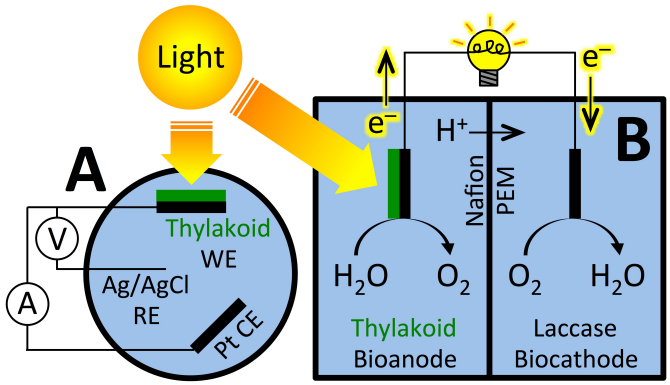


Fig. 2. A schematic diagram of thylakoid-bioanode-based device architectures used for this work. (A) The three-electrode electrochemical cell. WE: Working electrode; RE: Reference electrode; CE: Counter electrode. Note that the WE and CE are analogous to an anode and cathode, respectively. Also note that a potential is poised between the WE and RE, while current is allowed to flow at the WE and CE, as controlled by a potentiostat (not pictured). (B) The two-chamber bio-solar cell. A Nafion® proton exchange membrane (PEM) allows for charge balance during electron flow. Note that the thylakoid bioanode is identical to the WE in the three-electrode device.

abundant natural biological membrane—that is densely packed (~70% by area[14]) with photo- and electro-active protein complexes that convey energy *via* FRET.[15] One key thylakoid membrane protein complex is Photosystem II (PSII), a photosynthetic reaction center (RC) containing numerous antenna pigment molecules that absorb light and transfer photoexcitation energy to the P680 chlorophyll *a* (chl*a*) special pair at >90% efficiency.[16–21] This generates the P680* excited state (the primary electron donor in photosynthesis[16,22]) that is rapidly oxidized to $P680^+$ (the strongest naturally-occurring biological oxidant[16]) at near-unity quantum efficiency.[23] $P680^+$ drives water oxidation—evolving $O_2$, $4H^+$, and $4e^-$—in the metalloenzyme core of PSII,[15,18,21] so PSII is the primary source of usable electrons in thylakoid membranes.

In addition to PSII, Photosystem I (PSI) and the RCs from photosynthetic bacteria also exhibit quantum efficiencies approaching unity for photoexcitation energy transduction and charge separation.[24–27] There has therefore been keen effort in isolating these RCs and interfacing them with electrodes for photobioelectrochemical devices.[28–36] A related method (that is utilized in this manuscript) is the electrode immobilization of whole thylakoid membranes that naturally contain PSI and PSII. This requires fewer purification steps and allows better RC stability at the expense of some charge transfer efficiency. Herein, immobilization is accomplished *via* silica encapsulation with catalase,[37] though thylakoid membranes may also be "wired" to osmium redox polymers,[38] suspended with gold nanoparticles and quinones,[39] frozen in an albumin matrix,[40] incorporated in electrochemical cells with various mediators,[41] or tethered to multiwalled carbon nanotubes (MWCNTs).[42] These approaches, and more, have been critically reviewed.[43,44]

Two-compartment bio-solar cells constructed from spinach thylakoid bioanodes and laccase biocathodes were recently reported.[45,46] The thylakoid active layer absorbs light and generates electrons that are harvested as anodic photocurrent. This platform has been used to investigate additions of carbon quantum dots that sensitize thylakoid bio-solar cells[47] by increasing the direct electron transfer surface area of the electrode (increased current collection) and increasing absorbance and photoluminescence intensities (enhanced light harvesting). These devices have also been modified with the discussed quinone derivatives[39] and MWCNTs.[48] The thylakoid bioanodes of these devices have practical utility in biosensors,[40,49–52] photosensors,[53] and biotransistors.[54] Thus, improving their electrochemical performance is anticipated to enhance their sensitivity and applicability across a wide range of applications.

Herein, thylakoid bioanodes have been modified with the seven derivatives in Fig. 1 by directly adding COEs to the thylakoid suspensions during electrode construction. The resulting thylakoid/COE electrodes were employed in both three-electrode electrochemical cells (Fig. 2A) and bio-solar cells (Fig. 2B). As can be seen in the Fig. 2 schematic, the two-compartment design of the bio-solar cells allows use of two solutions so that COEs are prevented by the PEM from interacting with the cathode.[45] Because of the strong affinity of COEs for lipid bilayers,[1,55] it is reasonable to expect that thylakoid membrane proteins (*e.g.* PSII) and their bound pigments may be spatially proximate[56] to intercalated COE molecules and experience COE-induced optoelectronic and/or diffusion-related[57] changes. However, due to the essential influence of light reactions in this novel thylakoid/COE-testing platform, COEs are not necessarily expected to evoke the same functionality or electrical outputs as have previously arisen in non-illuminated microbial systems.[1–8] Therefore, this study is an essential conceptual steppingstone towards understanding practical utility of COEs in light-driven systems.

The manuscript is organized as follows. First, thylakoid/COE electrodes are characterized and optimized in a three-electrode device. Then, with all seven COE derivatives, optimized electrodes are used for photoamperometry in similar three-electrode devices and subsequently employed in bio-solar cell devices. The resulting device outputs are then statistically compared to establish photobioelectrochemical structure-property relationships. These experiments offer insight into the ideal combination of molecular structure and pendant charge functionality of COEs for enhancing the performance of practical thylakoid-bioanode-based devices.

## Results and Discussion

### Electrochemical characterization of thylakoid bioanodes and optimization of COE concentration

In a three-electrode device (see Fig. 2A, previous work,[46] and Experimental), thylakoid/COE electrodes containing 10 μM of each COE were first examined using cyclic voltammetry (CV) to identify electrochemical differences relative to unmodified thylakoid electrodes.

An example of the CV data is shown in Fig. S2 (ESI), specifically comparing the potential dependence of current output from an unmodified thylakoid electrode to a

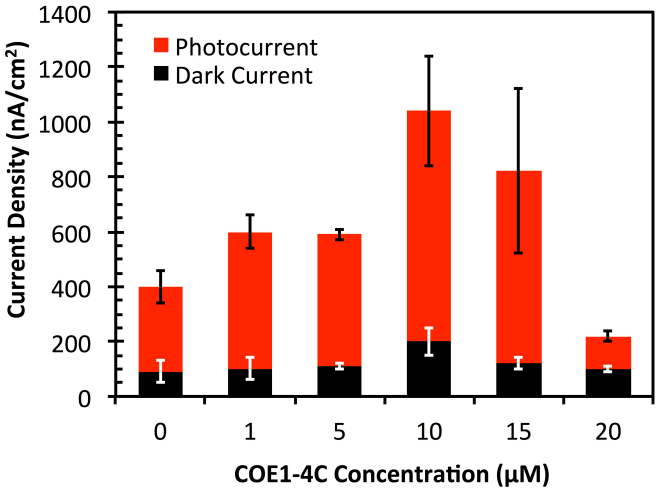


Fig. 3. Optimization of COE concentration for maximal current output. Measurements were conducted by amperometry at a poised potential of $E$ = 0.45 V vs. Ag/AgCl in 0.1 M, pH = 7.4 phosphate buffer. Photocurrent and dark current are presented stacked to illustrate the light current produced for each experimental condition (light current = dark current + photocurrent). Error bars represent ± 1 std. dev.

representative thylakoid/COE1-4C electrode. This was repeated for all tested COEs (not shown), and these data indicate that essentially no voltammetric difference exists between thylakoid/COE electrodes and unmodified thylakoid electrodes. Therefore, COEs are not contributing to anodic current *via* redox activity or chemical degradation. A small, reversible redox wave is identifiable in all CV traces at a central potential of ~0.35 V for thylakoid electrochemistry; all subsequent amperometric experiments were therefore conducted at $E$ = 0.45 V to allow oxidation of this redox species.

Using a similar three-electrode device, the COE concentration that maximizes current output from thylakoid/COE electrodes was identified amperometrically using COE1-4C. These experiments provide the current generated during a specific period of time (see Experimental). As can be seen in Fig. 3, a range of 1–20 μM COE1-4C was tested, which mimics the range typically explored in previous biological studies.[3–5,58] This range is equivalent to 50–1000 pmol COE per 50 μL solution, or 100–2000-fold less than the chlorophyll concentration in the thylakoid suspensions used for constructing the electrodes (see Experimental). The resulting amperometric light-, dark-, and photocurrent responses are summarized in Fig. 3. Dark current density is not significantly affected by the COE1-4C concentration, aside from a small increase at 10 μM COE1-4C. However, photocurrent density changes with COE1-4C concentration, as it increases slightly for 1 μM and 5 μM, maximizes at 10 μM, remains elevated at 15 μM, and then at 20 μM falls below unmodified (0 μM) thylakoid electrodes. From these data, 10 μM was chosen as the standard concentration for subsequent experiments.

### Amperometry reveals COE-induced thylakoid photocurrent enhancements

In Fig. 4, a representative example of amperometric current

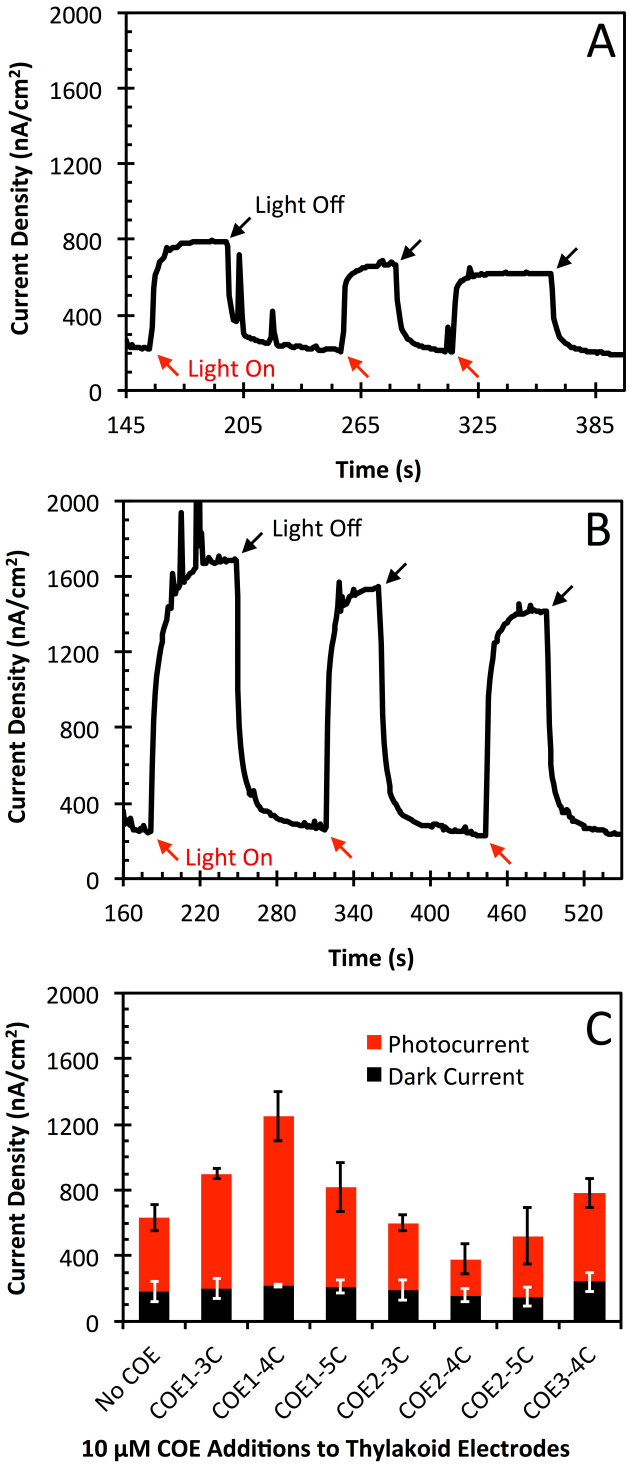


Fig. 4. Amperometric current measurements. All data were collected at 0.45 V vs. Ag/AgCl in 0.1 M, pH = 7.4 phosphate buffer. Red arrows indicate when the light was turned on and black arrows when it was turned off. (A) Representative time course of current density output from an unmodified (No COE) thylakoid electrode under modulated illumination. (B) Representative time course of current density output from a thylakoid/COE1-4C electrode under modulated illumination. (C) Summary of triplicate average current density outputs from thylakoid and thylakoid/COE electrodes for all tested COEs. In all cases, light current is equivalent to the sum of photocurrent (red) and dark current (black). Error bars are ± 1 std. dev.

Table 1. Amperometric current density measurements at $E$ = 0.45 V vs. Ag/AgCl with 10 μM COE additions in 0.1 M pH = 7.4 phosphate buffer

| 10 μM COE Additions to Thylakoids | Light Current | | | Dark Current | | | Photocurrent | | |
|---|---|---|---|---|---|---|---|---|---|
| | Density (μA/cm$^2$) | Fold Change | $p$-value[a] | Density (μA/cm$^2$) | Fold Change | $p$-value[a] | Density (μA/cm$^2$) | Fold Change | $p$-value[a] |
| No COE | 630 ± 120 | – | 1.000 | 180 ± 60 | – | 1.000 | 450 ± 80 | – | 1.000 |
| COE1-3C | 900 ± 20 | 1.4 ± 0.2 | 0.065* | 200 ± 60 | 1.1 ± 0.5 | 0.704 | 700 ± 30 | 1.6 ± 0.2 | 0.046** |
| COE1-4C | 1250 ± 160 | 2.0 ± 0.5 | 0.059* | 220 ± 10 | 1.2 ± 0.3 | 0.383 | 1030 ± 150 | 2.3 ± 0.8 | 0.010*** |
| COE1-5C | 820 ± 170 | 1.3 ± 0.4 | 0.360 | 210 ± 40 | 1.2 ± 0.4 | 0.640 | 610 ± 150 | 1.4 ± 0.5 | 0.204 |
| COE2-3C | 600 ± 100 | 1.0 ± 0.2 | 0.833 | 190 ± 60 | 1.1 ± 0.5 | 0.848 | 410 ± 50 | 0.9 ± 0.2 | 0.628 |
| COE2-4C | 390 ± 120 | 0.6 ± 0.2 | 0.070* | 160 ± 40 | 0.9 ± 0.4 | 0.751 | 220 ± 90 | 0.5 ± 0.2 | 0.143 |
| COE2-5C | 530 ± 200 | 0.8 ± 0.3 | 0.620 | 150 ± 60 | 0.8 ± 0.4 | 0.573 | 370 ± 170 | 0.8 ± 0.4 | 0.504 |
| COE3-4C | 790 ± 70 | 1.3 ± 0.2 | 0.257 | 240 ± 60 | 1.3 ± 0.6 | 0.288 | 540 ± 90 | 1.2 ± 0.3 | 0.454 |

[a] Calculated with 2-tailed $t$-tests comparing mean current densities of thylakoid/COE electrodes to unmodified thylakoid electrodes.
* Current density different than unmodified thylakoids at ≥ 90% significance ($p$ < 0.1)
** Current density different than unmodified thylakoids at ≥ 95% significance ($p$ < 0.05)
*** Current density different than unmodified thylakoids at ≥ 99% significance ($p$ < 0.01)

output from a 3-electrode device for an unmodified thylakoid electrode (Fig. 4A) is compared to the current output from a representative electrode modified with COE1-4C (Fig. 4B). The COE1-4C addition increases light current ("Light On" state) by approximately 2-fold, while dark current ("Light Off" state) is essentially unchanged; photocurrent is light minus dark current, so photocurrent increases about 3-fold in this specific instance. Triplicate average data and statistical significance for all COEs is summarized in Fig. 4C and Table 1 and discussed below.

From Table 1, three COE derivatives have a statistically significant effect on thylakoid light current output (at > 90% significance): COE1-3C, COE1-4C, and COE2-4C. Relative to unmodified thylakoids, addition of COE1-3C provides a 1.4 ± 0.2-fold increase in light current ($p$ = 0.065), and COE1-4C addition enables a 2.0 ± 0.5-fold increase in light current ($p$ = 0.059). However, COE2-4C makes the device worse, decreasing light current to 0.6 ± 0.2-fold ($p$ = 0.070). Dark current of thylakoid/COE electrodes is not statistically significantly different than the unmodified thylakoid electrodes for any tested COEs.

Photocurrent is statistically significantly higher (at ≥ 95% significance) with COE1-4C (2.3 ± 0.8-fold, $p$ = 0.010) and COE1-3C (1.6 ± 0.2-fold, $p$ = 0.046). This agrees with light current data because dark current is statistically unchanged. It is also noteworthy that by this 3-electrode technique, COE1-3C, COE1-4C, COE1-5C, and COE3-4C qualitatively increase the average measured photocurrent while COE2-3C, COE2-4C, and COE2-5C decrease it. This trend hints at COE molecular structural features playing a relevant photobioelectrochemical role that is further exposed in bio-solar cell experiments, below.

**Bio-solar cell experiments reveal statistically significant COE photobioelectrochemical structure-property relationships**

The same bioanode electrodes were accordingly employed in two-compartment bio-solar cells[45] to further probe whether the amperometric trends hold and whether COEs improve (a) photocurrent generation within the thylakoids or (b) the thylakoid-electrode contact for current harvesting—or a combination of (a) and (b). An example of the obtained solar cell data is shown in Fig. 5, comparing linear polarization (LP) traces of unmodified thylakoid bio-solar cells (Fig. 5A) to the best-performing thylakoid/COE1-4C devices (Fig. 5B).

Four COE derivatives afford a statistically significant increase to the bio-solar cell short circuit light current (light-$J_{sc}$): COE1-3C, COE1-4C, COE1-5C, and COE2-5C. Light-$J_{sc}$ is the sum of the contributions from short circuit dark current (dark-$J_{sc}$) and short circuit photocurrent (photo-$J_{sc}$). The best overall performance enhancement is afforded by COE1-4C, with a statistically significant 1.4-fold increase in each of light-$J_{sc}$, dark-$J_{sc}$, and photo-$J_{sc}$ ($p$ = 0.023, 0.030, and 0.055, respectively). This indicates that COE1-4C enhances *both* photocurrent generation and the thylakoid-electrode contact. It is worth noting that the dark current in Fig. 5B is also increased relative to the dark current in Fig. 5A at intermediate potentials

Table 2. Bio-solar cell $J$-$V$ characteristics by linear polarization at 5 mV/s with 10 μM COE additions

| | | 10 μM COE Additions to Thylakoids | | | | | | | |
|---|---|---|---|---|---|---|---|---|---|
| | | No COE | COE1-3C | COE1-4C | COE1-5C | COE2-3C | COE2-4C | COE2-5C | COE3-4C |
| Light Current | $V_{oc}$ (mV) | 699 ± 7 | 692 ± 6 | 691 ± 2 | 698 ± 4 | 684 ± 4 | 686 ± 1 | 682 ± 2 | 688 ± 7 |
| | $p$-value[a] | 1.000 | 0.259 | 0.130 | 0.215 | 0.032** | 0.033** | 0.016** | 0.127 |
| | $J_{sc}$ (μA/cm$^2$) | 10.2 ± 0.5 | 12.9 ± 1.1 | 14.3 ± 0.6 | 12.7 ± 1.0 | 11.2 ± 1.2 | 11.5 ± 1.0 | 12.1 ± 0.6 | 11.3 ± 1.0 |
| | Fold Change | - | 1.3 ± 0.2 | 1.4 ± 0.1 | 1.3 ± 0.1 | 1.1 ± 0.1 | 1.1 ± 0.1 | 1.2 ± 0.1 | 1.1 ± 0.1 |
| | $p$-value[a] | 1.000 | 0.032** | 0.023** | 0.031** | 0.3688 | 0.1386 | 0.089* | 0.183 |
| Dark Current | $V_{oc}$ (mV) | 695 ± 11 | 687 ± 9 | 688 ± 4 | 695 ± 6 | 683 ± 5 | 671 ± 3 | 668 ± 17 | 674 ± 12 |
| | $p$-value[a] | 1.000 | 0.385 | 0.359 | 1.000 | 0.161 | 0.022** | 0.082* | 0.090* |
| | $J_{sc}$ (μA/cm$^2$) | 7.9 ± 0.5 | 10.8 ± 0.5 | 11.2 ± 0.5 | 9.4 ± 1.2 | 8.4 ± 1.0 | 8.5 ± 1.8 | 9.0 ± 0.5 | 7.4 ± 1.2 |
| | Fold Change | - | 1.4 ± 0.1 | 1.4 ± 0.1 | 1.2 ± 0.2 | 1.1 ± 0.2 | 1.1 ± 0.3 | 1.1 ± 0.1 | 0.9 ± 0.2 |
| | $p$-value[a] | 1.000 | 0.039** | 0.030** | 0.208 | 0.507 | 0.669 | 0.194 | 0.597 |
| Photo-current | $J_{sc}$ (μA/cm$^2$) | 2.3 ± 0.1 | 2.1 ± 0.8 | 3.1 ± 0.3 | 3.3 ± 0.3 | 2.8 ± 0.5 | 3.0 ± 0.9 | 3.2 ± 0.4 | 3.9 ± 0.5 |
| | Fold Change | - | 0.9 ± 0.3 | 1.4 ± 0.2 | 1.5 ± 0.2 | 1.2 ± 0.3 | 1.3 ± 0.5 | 1.4 ± 0.3 | 1.7 ± 0.4 |
| | $p$-value[a] | 1.000 | 0.717 | 0.055* | 0.026** | 0.221 | 0.270 | 0.071* | 0.028** |

*a*. Calculated from 2-tailed $t$-tests comparing thylakoid/COE electrodes to unmodified thylakoid electrodes
*$J_{sc}$ different than unmodified thylakoids at ≥ 90% significance ($p$ < 0.1)
**$J_{sc}$ different than unmodified thylakoids at ≥ 95% significance ($p$ < 0.05)

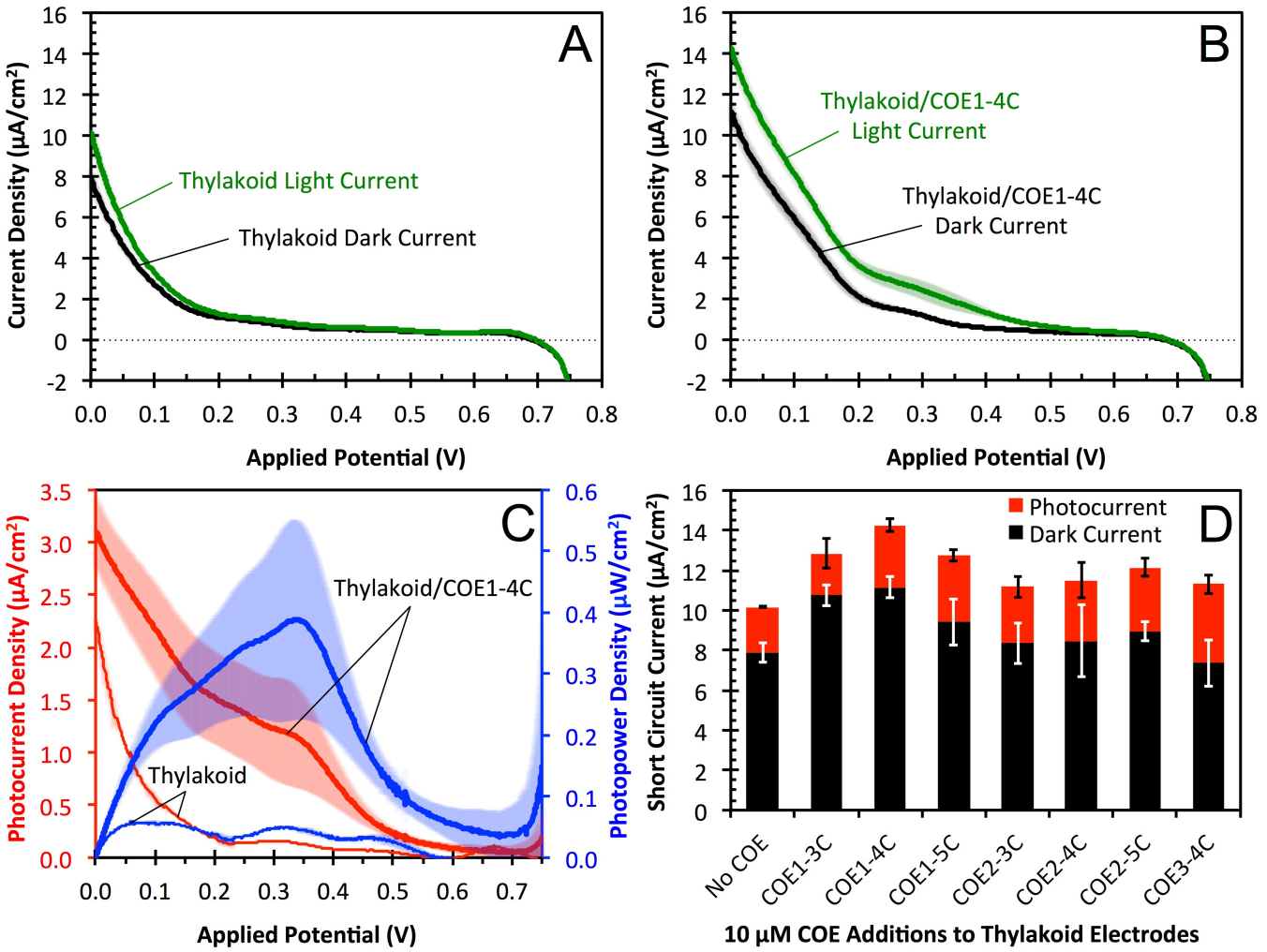


Fig. 5. Bio-solar cell data from linear polarization. Devices were operated with 0.1 M pH = 7.4 phosphate buffer in the anode chamber and 0.1 M, pH = 5.5 Na-citrate buffer in the cathode chamber. Colored shaded regions surrounding plotted data represent ± 1 std. dev. at each potential (in some instances, the error is smaller than the width of the line). Potential was swept at 5 mV/s. (A) Average dark and light *J-V* curves for unmodified thylakoid bio-solar cells. (B) Average dark and light *J-V* curves for the highest-performing thylakoid/COE1-4C bio-solar cells. (C) Average photocurrent density (red) and photopower density (blue) measurements as a function of applied potential for devices in A and B. Here, photocurrent was calculated by subtracting dark current from light current for each of three devices and then taking the average. Photopower density is provided by $P = JV$. (D) Summary of dark-$J_{sc}$ (black), photo-$J_{sc}$ (red), and light-$J_{sc}$ (red + black) for thylakoid and thylakoid/COE bio-solar cells for all tested COEs. Error bars represent ± 1 std. dev.

in the range 0 V < E ≤ 0.35 V. This increase in current indicates a decrease in device resistance that is consistent with the COE improving the thylakoid-electrode electrical contact. Fig. 5C displays photo-$J_{sc}$ (red) and photo-power density (blue) for these representative devices, and in this instance, COE1-4C increases photopower about an order of magnitude at the maximum power point near +0.35 V applied potential. COE1-3C, COE1-5C, and COE2-5C also furnish statistically significant increases in light-$J_{sc}$ of 1.3 ± 0.2-fold ($p$ = 0.032), 1.3 ± 0.1-fold ($p$ = 0.031), and 1.2 ± 0.1-fold ($p$ = 0.089), respectively. $J_{sc}$ data is summarized in Fig. 5D, and a numerical summary with statistical significance of all data may be found in Table 2.

For COE1-3C, the increase in light-$J_{sc}$ stems primarily from a 1.4 ± 0.1-fold (p = 0.039) increase in dark-$J_{sc}$ and no significant change in photo-$J_{sc}$; this implicates an improved electrode contact as the primary reason for current enhancement. For COE1-5C, the increase in light-$J_{sc}$ arises from a 1.5 ± 0.2-fold ($p$ = 0.026) increase in photo-$J_{sc}$, but no change to dark-$J_{sc}$. These results suggest that COE1-5C enables enhanced photocurrent generation. It is also worth noting that for these COE1-type derivatives, the open circuit voltage under illumination (light-$V_{oc}$) and in the dark (dark-$V_{oc}$) remain statistically indistinguishable. Finally, for COE2-5C, the 1.2 ± 0.1-fold ($p$ = 0.089) light-$J_{sc}$ increase results from a 1.4 ± 0.3-fold ($p$ = 0.071) increase in photo-$J_{sc}$, without a dark-$J_{sc}$ increase, again implicating enhanced photocurrent generation.

For COE2-3C and COE2-4C, average dark-$J_{sc}$ and photo-$J_{sc}$ increase slightly, but it is not statistically significant. For COE3-4C, the lack of change in light-$J_{sc}$ appears to occur because of offsetting positive and negative effects: dark-$J_{sc}$ decreases slightly, concomitant with a statistically significant 1.7 ± 0.4-fold ($p$ = 0.028) increase in photo-$J_{sc}$, eliciting the highest photocurrent of any COE tested (3.9 ± 0.5 μA/cm$^2$).

From Table 2, three photobioelectrochemical structure-property relationships emerge: (i) COE1-3C, COE1-4C, and COE1-5C cause light-$J_{sc}$ to increase at 95% significance. The key difference in these molecules is that the chromophore structures bear distal N heteroatoms (Fig. 1). The efficacy of COE1-type molecules over COE2-type points to a relevant photobioelectrochemical role for the N atoms. (ii) Shorter COEs (COE1-3C, COE1-4C) allow significantly better dark current collection by the bioanode, presumably by directly modifying the thylakoid-electrode interface (*via* membrane intercalation[55]), thereby improving the contact. Longer COEs (COE1-4C, COE1-5C, COE2-5C, COE3-4C) enhance photocurrent generation. COE1-4C appears to have the best mixture of these length-dependent characteristics. (iii) Structurally, COE3-4C and COE1-4C differ only in their pendant charged groups. Whereas COE1-4C bears cationic groups and significantly increases thylakoid bioanode current outputs, COE3-4C bears anionic groups and only increases photocurrent outputs. This signifies that the pendant cationic moieties impact increased dark current outputs in this system.

## Experimental

### Thylakoid extraction, chlorophyll content, and photoactivity

For this work, thylakoid membrane suspensions were obtained from fresh organic spinach, evaluated for chlorophyll content, and validated as active by established protocols.[37,45,48] The entire procedure is explained here and was conducted at 4°C. Organic spinach from a local supermarket was washed with ultrapure water and dried. Three aqueous solutions were prepared for thylakoid extraction and electrode deposition: (1) Extraction buffer (5X) contained 300 g/L D-sorbitol, 62.5 g/L 2-[4-(2-hydroxyethyl)piperazin-1-yl]ethanesulfonic acid (HEPES), 2.9 g/L NaCl, 3.7 g/L ethylenediaminetetraacectic acid disodium dehydrate (EDTA), and 10 g/L $MgCl_2$; this was then diluted 5X to make a working extraction buffer. (2) Lysing solution contained 0.19 g/L $MgCl_2$. (3) Deposition buffer (pH = 7.8) contained 60 g/L D-sorbitol, 11.9 g/L HEPES, and 0.19 g/L $MgCl_2$, as well as 1 µL of a commercial 272.1 kU/mL (28.7 mg/mL) *Aspergillus niger* catalase suspension (Sigma Aldrich) per 100 µL of solution.

Spinach was deveined and blended for five pulses of 5 seconds in working extraction buffer. The resultant mixture was filtered through three layers of cheesecloth and supernatant was retained. Supernatant was centrifuged at 200×g for 3 minutes to remove cellular debris. Debris-free supernatant was transferred and centrifuged at 1000×g for 7 minutes to pellet chloroplasts. Supernatant was discarded, and chloroplasts were resuspended in a minimal volume of working extraction buffer; this was gently pipetted onto a 40% Percoll® density gradient (60% working extraction buffer) and centrifuged for 6 minutes at 1700×g. The resulting pellet was lysed in lysing solution for 30 seconds to extract thylakoids and then immediately resuspended in deposition buffer. If not immediately used, these thylakoid suspensions were stored at −20°C.

By measuring the absorbances of the thylakoids in deposition buffer at 645 nm ($A_{645}$) and 663 nm ($A_{663}$), then using these values in a previously reported equation for chlorophyll *a* (chl*a*) concentration, given[48] [chl*a*] (mg/ml) = $(8.02A_{663} + 20.2A_{645})/10$, and finally multiplying by the molar mass of chl*a* (893.5 g/mol), chlorophyll content was determined to be ~100 nmol chlorophyll per 50 µL of thylakoid suspension, or ~2 mM. As discussed in the main text, this is 200-fold more concentrated than 10 µM COE additives.

In order to validate their photoactivity, extracted thylakoids were immobilized from deposition buffer onto a glass coverslip and oxygen production was measured using a micro-dissolved oxygen probe from Shelfscientific. The coverslip was immersed in 5 mL of 0.1 M phosphate buffer (pH = 7.4) containing 0.1 M nitrate, and oxygen concentration was measured in the dark until a stable value was obtained; the measurement was repeated while illuminating the coverslip-immobilized thylakoids. With confirmed thylakoid oxygen production (photoactivity), thylakoid electrodes were then fabricated according to previously reported procedures;[45] this is also described in the next section.

### Fabrication of thylakoid bioanodes and laccase biocathodes

3 cm × 1 cm pieces of Toray® carbon paper were first excised with a razor. A further 2 cm × 0.2 cm section was removed from the corner of each piece, and the retained 2 cm × 0.8 cm section was coated in wax to leave a 1 cm × 1 cm electroactive surface.

For thylakoid bioanodes, 50 µL of the thylakoid suspensions (in deposition buffer) were pipetted and spread onto one side of the 1 cm × 1 cm section and allowed to air dry for 30 minutes. Fig. S3A (ESI) depicts several of these electrodes in the drying stage. In a fume hood, dried electrodes were placed with a thimbleful of tetramethyl orthosilicate and covered with a glass petri dish for 15 minutes to create a silica coating on the thylakoids.[37] These completed electrodes were stored at 4°C overnight and used the next day. Thylakoid/COE electrodes were fabricated the same way, except that the desired COE concentration was added homogeneously with light agitation to 50 µL of the thylakoid suspension immediately prior to pipetting onto the carbon paper working electrode.

For laccase biocathodes, 15 mg of previously-prepared anthracene-modified multiwalled carbon nanotubes[59] were mixed with 150 mL purified laccase solution (Amano Enzyme, Inc.). This mixture was vortexed, then sonicated for 10 min, and this was repeated a second time. A 50 mL aliquot of tetrabutylammonium bromide-modified Nafion® from an established procedure[60] was then added to the mixture, followed by an additional 5 minutes of vortexation. The resulting thin black mixture was painted onto the 1 cm × 1 cm electroactive section and allowed to dry for ~30 min.

### Cyclic voltammetry

Scans were performed in a three-electrode electrochemical cell (Fig. 2A and Fig. S3B, ESI), with each prepared electrode condition, in triplicate, in both the dark and the light. The



 

electrolyte was 100 mM, pH = 7.4 phosphate buffer. Working electrodes were thylakoid electrodes, and electrical contact was made in the wax-coated section by clamping through the wax with an alligator clip; the reference electrode was Ag/AgCl (saturated KCl); the counter electrode was platinum mesh. Potential was swept twice from −100 mV to 650 mV at 5 mV/s, and the second sweep from each scan was recorded. All photoelectrochemical measurements of working electrodes were obtained with a CH Instruments CHI660 electrochemical workstation. Representative results from these experiments for unmodified thylakoids and COE1-4C-modified thylakoids are presented in Fig. S2 (ESI). Remaining traces of all other tested conditions are featureless and are essentially no different than these traces; therefore, they are omitted for the sake of clarity. The Toray® carbon paper working electrode has a very high surface area that leads to high capacitive currents, and this accounts for the large difference in current in forward and reverse scans (~2 μA/cm$^2$) in these CV experiments. The increase in current above E = 0.5 V is due to the electrochemistry of the electrode and not the thylakoids or COEs, which was confirmed by control CV scans of bare carbon electrodes (not shown).

**Amperometry**

Current collection was performed at 0.45 V vs. Ag/AgCl in a three-electrode electrochemical cell (Fig. S3B, ESI) with 100 mM, pH = 7.4 phosphate buffer as the electrolyte. Working electrodes were thylakoid electrodes, and electrical contact was made in the wax-coated section by clamping through the wax with an alligator clip; the reference electrode was Ag/AgCl (saturated KCl); the counter electrode was platinum mesh. All photoelectrochemical measurements were obtained with a CH Instruments CHI660 electrochemical workstation. The current output from thylakoid (working) electrodes was monitored continuously, first in the dark until stable (~60 s) and then under illumination until stable (~60 s); this on-off switching was repeated three times in succession for each tested electrode and then averaged. The light current, dark current, and photocurrent densities were recorded as such and averaged for each experimental condition in triplicate. The light source was a 250 W (5200 lumen) halogen lamp positioned ~20 cm away from the electrode surface (see Fig. S3C, ESI).

**Bio-solar cells**

Two-chamber bio-solar cells were implemented with the thylakoid/COE electrodes, a laccase biocathode, and a Nafion® 212 proton exchange membrane, as previously reported.[45] Briefly, the solar cell device was constructed from four layered 5 cm × 5 cm × 0.5 cm pieces of poly(methyl methacrylate) bolted together. The two central pieces have a hole milled from the center and a slot milled outward from this hole at the top of the piece, allowing electrodes to be inserted into each (see Fig. S3C, ESI). The two central pieces are separated by the Nafion®, which importantly allows for each compartment to be filled with different solutions, as each electrode operates optimally at a different pH in this device: the anode compartment was filled with ~3 mL of 100 mM, pH 7.4 phosphate buffer, while the cathode compartment contained ~3 mL of 150 mM, pH 5.5 citrate buffer. Anode-cathode separation was thus ~1 cm.

Linear polarization (LP) was used to obtain dark and light current-potential (*J-V*) curves for the solar cells, and the photocurrent was calculated from the difference in the curves. In LP (also commonly referred to as linear sweep voltammetry, or LSV), the potential between the anode and cathode is varied (without a reference electrode), while current is monitored, allowing for probing of light and dark *J-V* characteristics of the devices. LP experiments were performed using a Digi-IVY DY2023 potentiostat. Illumination was provided by a 250 W (5200 lumen) halogen lamp positioned ~20 cm away from the electrode. For each triplicate set of electrodes, the average short circuit current density and open circuit voltage were determined from the y- and x-intercepts of the *J-V* curves, respectively.

**Ultraviolet-visible (UV-vis) absorbance spectroscopy**

In a quartz cuvette with 1 cm path length, aqueous absorbance measurements were conducted at 1 nm wavelength intervals (20 nm/s) in the range 250–800 nm (Beckman Coulter DU 800 Spectrophotometer). An absorbance versus [COE] calibration curve was generated by measuring UV-vis spectra for the various COEs at a series of concentrations. By identifying the wavelength of maximal absorption ($\lambda_{max}$), plotting the absorbance intensity at $\lambda_{max}$ as a function of the concentration, and fitting these data by least squares, a straight line through the origin was generated with slope equal to the extinction coefficient ($\varepsilon$) of each COE derivative. An example of this data for COE1-4C is provided in Fig. S4, ESI.

## Conclusions

For the first time, certain COEs have been shown to improve electrical contacts and photocurrent generation in thylakoid-membrane-based photobioelectrochemical devices. The chemical features associated with these enhancements have been determined by systematic variation of the added COE molecules, and we imagine that these results have the potential to extend to other subcellular light-driven systems. COE1-4C appears to have the most ideal combination of molecular structure and pendant charge functionality, making it the recommended derivative for use in practical photobioelectrochemical devices. Amperometric and bio-solar cell data highlight several conclusions regarding these COE properties, as follows.

Within the class of compounds studied here, the molecular length of COE1-4C appears to be the most ideally suited to enhance thylakoid dark- and photo-current outputs, as compared to its shorter and longer counterparts (COE1-3C and COE1-5C, respectively). This agrees with similar observations in microbial systems that produce dark current.[1,4] Lipid bilayer modelling studies help rationalize this, suggesting that COE1-3C may aggregate and harmfully pinch a membrane to a greater degree than COE1-4C.[55] However, considerations of molecular length are insufficient as a direct design element for estimating

biocurrent performance impact. Consider that COE1-4C and COE2-4C have similar lengths, and yet we point out that their photobioelectrochemical effects on thylakoids are different. Due to optoelectronic differences in their chromophores, these molecules may have tendencies to accumulate in subtly different locations within the complex thylakoid membrane suspensions, thereby differentiating their ability to influence the thylakoid-electrode contact. An improved contact when using COE1-type molecules, as compared to COE2-type molecules, would aid in photocurrent collection, thus enabling the observed enhanced photobioelectrochemical energy conversion. The situation between COE1-4C and COE3-4C, which also have similar dimensions, is discussed in more detail below.

COE1-4C bears quaternary ammonium pendant groups, while COE3-4C bears carboxylate pendant groups, and both molecules have the same π-conjugated phenylenevinylene chromophore with distal N atoms. COE1-4C and COE3-4C will therefore have opposite coulombic interactions with charged surfaces, while keeping the conjugated segment constant. The thylakoid membrane surface carries a net negative charge from carboxylate moieties,[61] so thylakoid/COE3-4C coulombic repulsion should limit COE3-4C incorporation in the membrane. This reasoning is bolstered by new research showing that COE3-4C does not spontaneously intercalate into bacterial membranes (which are also negatively charged), nor does it enhance dark current extraction from bacteria, and these appear to be strongly correlated.[8] Indeed, in this present work, COE3-4C does not increase the thylakoid dark current (while COE1-4C does), and yet both COE1-4C and COE3-4C increase photocurrent. These results are consistent with the proposed differences in the location of accumulation in the thylakoid matrix as a function of molecular structure.

## Acknowledgements

Funding was provided by the Institute for Collaborative Biotechnologies (ICB) under grant W911F-09-D-0001 from the U.S. Army Research Office. M. A. R. would like to acknowledge the National Science Foundation MRSEC (Grant #DMR 11-21252) for funding her postdoctoral fellowship. Content does not necessarily reflect the position or policy of the Government, and no official endorsement should be inferred. The authors would also like to thank Amano Enzyme, Inc. for the laccase used in this work.

## Notes and references

[a] Materials Department, University of California, Santa Barbara, California, CA 93106, USA.

[b] Department of Chemistry, University of Utah, 315 S 1400 E Rm 2020, Salt Lake City, UT 84112, USA. E-mail: minteer@chem.utah.edu; Tel: +1-801-587-8325

[c] Department of Chemistry and Biochemistry, University of California, Santa Barbara, CA 93106, USA. E-mail: bazan@chem.ucsb.edu; Tel: +1-805-893-5538

[d] Center of Excellence for Advanced Materials Research (CEAMR), King Abdulaziz University, Jeddah, Saudi Arabia

† Electronic Supplementary Information (ESI) available. See DOI: 10.1039/c000000x/

§ These authors contributed equally to this work.

1 L. E. Garner, J. Park, S. M. Dyar, A. Chworos, J. J. Sumner and G. C. Bazan, *J. Am. Chem. Soc.*, 2010, **132**, 10042–52.

2 L. E. Garner, A. W. Thomas, J. J. Sumner, S. P. Harvey and G. C. Bazan, *Energy Environ. Sci.*, 2012, **5**, 9449–9452.

3 V. B. Wang, J. Du, X. Chen, A. W. Thomas, N. D. Kirchhofer, L. E. Garner, M. T. Maw, W. H. Poh, J. Hinks, S. Wuertz, S. Kjelleberg, Q. Zhang, J. S. C. Loo and G. C. Bazan, *Phys. Chem. Chem. Phys.*, 2013, **15**, 5867–72.

4 H. Hou, X. Chen, A. W. Thomas, C. Catania, N. D. Kirchhofer, L. E. Garner, A. Han and G. C. Bazan, *Adv. Mater.*, 2013, 1–5.

5 A. W. Thomas, L. E. Garner, K. P. Nevin, T. L. Woodard, A. E. Franks, D. R. Lovley, J. J. Sumner, C. J. Sund and G. C. Bazan, *Energy Environ. Sci.*, 2013, **6**, 1761.

6 V. B. Wang, N. D. Kirchhofer, X. Chen, M. Y. L. Tan, K. Sivakumar, B. Cao, Q. Zhang, S. Kjelleberg, G. C. Bazan, S. C. J. Loo and E. Marsili, *Electrochem. commun.*, 2014, **41**, 55–58.

7 N. D. Kirchhofer, X. Chen, E. Marsili, J. J. Sumner, F. W. Dahlquist and G. C. Bazan, *Phys. Chem. Chem. Phys.*, 2014, **16**, 20436–43.

8 A. W. Thomas, C. Catania, L. E. Garner and G. C. Bazan, *Chem. Commun.*, 2015, **51**, 9294–9297.

9 Y. Lee, I. Yang, J. Lee and S. Hwang, *J. Phys. Chem. C*, 2013, **117**, 3298–3307.

10 T. Förster, *Ann. Phys.*, 1948, **6**, 55–75.

11 P. Beaujuge, C. Amb and J. R. Reynolds, *Acc. Chem. Res.*, 2010, **43**, 1396–1407.

12 S. H. Choi and C. D. Frisbie, *J. Am. Chem. Soc.*, 2010, **132**, 16191–201.

13 J. E. Coughlin, Z. B. Henson, G. C. Welch and G. C. Bazan, *Acc. Chem. Res.*, 2014, **47**, 257–70.

14 H. Kirchhoff, U. Mukherjee and H. Galla, *Biochemistry*, 2002, **41**, 4872–4882.

15 H. Dau and K. Sauer, *Biochim. Biophys. Acta - Bioenerg.*, 1996, **1273**, 175–190.

16 H. Dau and I. Zaharieva, *Acc. Chem. Res.*, 2009, **42**, 1861–70.

17 G. Krause and E. Weis, *Annu. Rev. Plant Physiol. Plant Mol. Biol.*, 1991, **42**, 313–349.

18 G. Raszewski, B. A. Diner, E. Schlodder and T. Renger, *Biophys. J.*, 2008, **95**, 105–19.

19 R. Kouřil, J. P. Dekker and E. J. Boekema, *Biochim. Biophys. Acta*, 2012, **1817**, 2–12.

20 J. Standfuss, A. C. Terwisscha van Scheltinga, M. Lamborghini and W. Kühlbrandt, *EMBO J.*, 2005, **24**, 919–28.

21 T. Renger and E. Schlodder, *J. Photochem. Photobiol. B.*, 2011, **104**, 126–41.

22 M. Grabolle and H. Dau, *Biochim. Biophys. Acta*, 2005, **1708**, 209–18.

23 P. J. Booth, B. Crystall, I. Ahmad, J. Barber, G. Porter and D. R. Klug, *Biochemistry*, 1991, **30**, 7573–7586.

24 C. A. Wraight and R. K. Clayton, *Biochim. Biophys. Acta*, 1974, **333**, 246–260.

25 A. J. Hoff and J. Deisenhofer, *Phys. Rep.*, 1997, **287**, 1–247.

26 L. O. Pålsson, C. Flemming, B. Gobets, R. van Grondelle, J. P. Dekker and E. Schlodder, *Biophys. J.*, 1998, **74**, 2611–2622.



 

27 S. W. Hogewoning, E. Wientjes, P. Douwstra, G. Trouwborst, W. van Ieperen, R. Croce and J. Harbinson, *Plant Cell*, 2012, **24**, 1921–1935.
28 G. LeBlanc, E. Gizzie, S. Yang, D. E. Cliffel and G. K. Jennings, *Langmuir*, 2014, **30**, 10990–11001.
29 H. Yaghoubi, Z. Li, D. Jun, R. Saer, J. E. Slota, M. Beerbom, R. Schlaf, J. D. Madden, J. T. Beatty and A. Takshi, *J. Phys. Chem. C*, 2012, **116**, 24868–24877.
30 H. Yaghoubi, Z. Li, D. Jun, E. Lafalce, X. Jiang, R. Schlaf, J. T. Beatty and A. Takshi, *J. Phys. Chem. C*, 2014, **118**, 23509–23518.
31 H. Yaghoubi, E. Lafalce, D. Jun, X. Jiang, J. T. Beatty and A. Takshi, *Biomacromolecules*, 2015, **16**, 1112–1118.
32 R. Das, P. J. Kiley, M. Segal, J. Norville, A. A. Yu, S. A. Trammell, L. E. Reddick, R. Kumar, F. Stellacci, N. Lebedev, J. Schnur, B. D. Bruce, S. Zhang, M. Baldo and L. Wang, *Nano Lett.*, 2004, **4**, 1079–1083.
33 P. O. Saboe, C. E. Lubner, N. S. McCool, N. M. Vargas-Barbosa, H. Yan, S. Chan, B. Ferlez, G. C. Bazan, J. H. Golbeck and M. Kumar, *Adv. Mater.*, 2014, **26**, 7064–7069.
34 E. Katz, *J. Electroanal. Chem.*, 1994, **365**, 157–164.
35 E. Y. Katz, A. Y. Shkuropatov, O. I. Vagabova and V. A. Shuvalov, *Biochim. Biophys. Acta - Bioenerg.*, 1989, **976**, 121–128.
36 R. Caterino, R. Csiki, A. Lyuleeva, J. Pfisterer, M. Wiesinger, S. D. Janssens, K. Haenen, A. Cattani-Scholz, M. Stutzmann and J. A. Garrido, *ACS Appl. Mater. Interfaces*, 2015, **7**, 8099–8107.
37 K. H. Sjoholm, M. Rasmussen and S. D. Minteer, *ECS Electrochem. Lett.*, 2012, **1**, G7–G9.
38 H. Hamidi, K. Hasan, S. C. Emek, Y. Dilgin, H.-E. Åkerlund, P.-Å. Albertsson, D. Leech and L. Gorton, *ChemSusChem*, 2015, **8**, 990–993.
39 K. Hasan, Y. Dilgin, S. C. Emek, M. Tavahodi, H.-E. Åkerlund, P.-Å. Albertsson and L. Gorton, *ChemElectroChem*, 2014, **1**, 131–139.
40 M. Purcell and R. Carpentier, *Biotechnol. Tech.*, 1990, **4**, 363–368.
41 M. Mimeault and R. Carpentier, *Enzyme Microb. Technol.*, 1988, **10**, 691–694.
42 J. O. Calkins, Y. Umasankar, H. O'Neill and R. P. Ramasamy, *Energy Environ. Sci.*, 2013, **6**, 1891–1900.
43 M. Rasmussen and S. D. Minteer, *J. Electrochem. Soc.*, 2014, **161**, H647–H655.
44 M. T. Giardi and E. Pace, *Trends Biotechnol.*, 2005, **23**, 257–263.
45 M. Rasmussen, A. Shrier and S. D. Minteer, *Phys. Chem. Chem. Phys.*, 2013, **15**, 9062–5.
46 M. Rasmussen and S. D. Minteer, *Phys. Chem. Chem. Phys.*, 2014, **16**, 17327–31.
47 M. Rasmussen, A. Wingersky and S. D. Minteer, *ECS Electrochem. Lett.*, 2014, **3**, H1–H3.
48 J. O. Calkins, Y. Umasankar, H. O'Neill and R. P. Ramasamy, *Energy Environ. Sci.*, 2013, **6**, 1891.
49 M. Rasmussen and S. D. Minteer, *Anal. Methods*, 2013, **5**, 1140–1144.
50 F. Bettazzi, S. Laschi and M. Mascini, *Anal. Chim. Acta*, 2007, **589**, 14–21.
51 M. Giardi, M. Koblízek and J. Masojídek, *Biosens. Bioelectron.*, 2001, **16**, 1027–1033.
52 R. Carpentier, C. Loranger, J. Chartrand and M. Purcell, *Anal. Chim. Acta*, 1991, **249**, 55–60.
53 N. Terasaki, N. Yamamoto, M. Hattori, N. Tanigaki, T. Hiraga, K. Ito, M. Konno, M. Iwai, Y. Inoue, S. Uno and K. Nakazato, *Langmuir*, 2009, **25**, 11969–74.
54 S. Fletcher, *J. Solid State Electrochem.*, 2015, **19**, 241–250.
55 J. Hinks, Y. Wang, W. H. Poh, B. C. Donose, A. W. Thomas, S. Wuertz, S. C. J. Loo, G. C. Bazan, S. Kjelleberg, Y. Mu and T. Seviour, *Langmuir*, 2014, **30**, 2429–40.
56 M. Pribil, M. Labs and D. Leister, *J. Exp. Bot.*, 2014, **65**, 1955–72.
57 H. Kirchhoff, *Biochim. Biophys. Acta*, 2014, **1837**, 495–502.
58 P. Gwozdzinska, R. Pawlowska, J. Milczarek, L. E. Garner, A. W. Thomas, G. C. Bazan and A. Chworos, *Chem. Commun.*, 2014, **50**, 14859–14861.
59 M. T. Meredith, M. Minson, D. Hickey, K. Artyushkova, D. T. Glatzhofer and S. D. Minteer, *ACS Catal.*, 2011, **1**, 1683–1690.
60 T. L. Klotzbach, M. Watt, Y. Ansari and S. D. Minteer, *J. Memb. Sci.*, 2008, **311**, 81–88.
61 J. Barber, *Annu. Rev. Plant Physiol.*, 1982, **33**, 261–295.

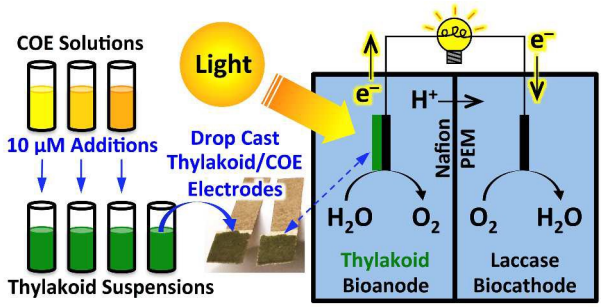


Systematic modification of thylakoid bioanodes with conjugated oligoelectrolytes reveals the structural features that increase photocurrent densities and improve electrode contacts in photobioelectrochemical devices.